Theor Chem Acc (1997) 96:31–38

Theoretical
Chemistry Accounts

Quantum dynamics study of Li + HF reaction

Wei Zhu, Dunyou Wang, John Z. H. Zhang

Department of Chemistry, New York University, New York, NY 10003, USA

Received: 8 January 1997 / Accepted: 14 January 1997

Abstract. We report rigorous quantum dynamics studies of the Li + HF reaction using the time-dependent wavepacket approach. The dynamics study is carried out on a recent ab initio potential energy surface, and state-selected reaction probabilities and cross sections are calculated up to 0.4 eV of collision energy. Many long-lived resonances (as long as 10 ps) at low collision energies (below 0.1 eV) are uncovered from the dynamics calculation. These long-lived resonances play a dominant role in the title reaction at low collision energies (below 0.1 eV). At higher energies, the direct reaction process becomes very important. The reaction probabilities from even rotational states exhibit a different energy dependence than those from odd rotational states. Our calculated integral cross section exhibits a broad maximum near the collision energy of 0.26 eV with small oscillations superimposed on the broad envelope which is reminiscent of the underlying resonance structures in reaction probabilities. The energy dependence of the present CS cross section is qualitatively different from the simple *J*-shifting approximation, in which a monotonic increase of cross section with collision energy was obtained.

Key words: Time-dependent approach – Wavepacket propagation – Integral cross section – Atom-diatom reactive scattering – Coupled state approximation

1 Introduction

The reaction of Li + HF has attracted much attention both theoretically [1–5] and experimentally [6–9]. This is an atom-diatom reaction with no identical atoms, and the reaction can be characterized as a light-heavy-light system. Ab initio potential energy surface calculations have been performed for this reaction [1–4], and results of a recent calculation [3] have been fitted to a global potential energy surface (PES) [5] for dynamics calculations. The potential energy surface for the Li + HF reaction has a nonlinear geometry at the saddle point with a potential barrier of 0.182 eV along the reaction path. There are two shallow potential wells, one in the entrance channel with a well depth of 0.302 eV and the other in the product channel with a well depth of 0.087 eV with respect to the reactant asymptote [5]. The reaction is exoergic by about 0.043 eV, including zero point energies. Figure 1 shows a contour plot of the PES as a function of the reactant Jacobi coordinates R and r for fixed angle θ between the Li–HF and HF vector of 74°, which includes the saddle point geometry. Early dynamics calculations employed classical trajectory methods [10] and approximate quantum methods [11–13]. More recently, three-dimensional quantum dynamics studies have been reported for the calculation of reaction probabilities at a total angular momentum J of 0 [5, 14] and of cross sections using the centrifugal sudden (CS) approximation at collision energies below 0.13 eV [15] on the PES of Ref. [5].

Recent 3D quantum dynamics calculations, both time-dependent [14] and time-independent [5, 15], have provided a wealth of dynamics information for Li + HF reaction. The hyperspherical coordinate calculation of Ref. [5] has produced state-selected reaction probabilities for $J = 0$ in the collision energy range between 0.004 and 0.35 eV. These probabilities show clear resonance features. The reaction probabilities from the TD calculation of Ref. [14] show a broad background structure with resonance features superimposed on it, and the reaction probabilities are sensitive to initial rotational states. Both calculations clearly indicate the presence of resonance in this reaction, but the results of the two are difficult to compare in detail. Baer et al. [15] have recently employed the CS approximation to calculate the reaction cross section at low energies (below 0.1 eV). Their calculated cross section shows maxima within the energy of their calculation [15]. However, no results of cross section are available from this calculation for energies above 0.13 eV, where an experimental measurement of cross section is available for comparison [7]. Lagana et al. [16] have recently calculated the reac-

Correspondence to: W. Zhu

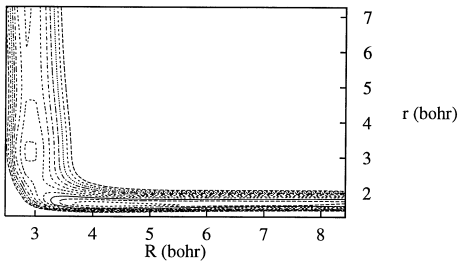

Fig. 1. Contour of the potential energy surface as a function of two radial Jacobi coordinates R (between Li and the center of HF) and r (HF distance) for a fixed angle θ of 74°

tion probabilities for zero total angular momentum ($J = 0$) using the hyperspherical coordinate method and employed a "J-shifting" approximation [17] to obtain cross sections based on the calculated reaction probabilities for $J = 0$. The resultant J-shifting cross section is a monotonically increasing function of collision energy throughout the energy range of their calculation. Since the "J-shifting" technique is a very crude approximation, the validity of the resultant cross section needs to be checked against more accurate calculations such as that of CS approximation.

In this study, we present a TD wavepacket study to calculate reaction probabilities and cross sections for the Li + HF reaction to investigate the dynamical features of this reaction, in particular resonances at all energies below 0.4 eV. Previous quantum dynamics calculations indicate that resonances are particular significant at low collision energies which is generally expected for reactions with wells. The present study also calculates integral cross sections using CS approximation to explicitly examine the effect of resonance on cross sections. The calculated reaction cross sections from the initial ground state are compared to that of the J-shifting approximation of Ref. [16] and with experimental results. The influence of initial rovibrational state on reaction probabilities is also investigated and its implications for the observed cross section are discussed.

This paper is organized as follows: Sect. 2 presents the general theory of the TD calculation for the Li + HF reaction. Section 3 presents the results of our calculation including state-selected reaction probabilities and cross sections as well as discussions of the results. Section 4 summarizes the present study.

2 Theory

Efficient TD wavepacket methods for calculating initial state-selected total (final state-summed) reaction probabilities have been developed recently for atom-diatom reactions [18] and diatom-diatom reactions [19, 20]. In these approaches, absorbing potentials V_p are employed to absorb the wavefunction to avoid boundary reflection of the wavefunction due to finite numerical grid [21]. If one does not need to resolve final states of the product, one can effectively use the reactant Jacobi coordinates to carry out the entire TD propagation of the wavefunction. If the final state distribution is desired, such a single coordinate method is not efficient and one should either switch to the product Jacobi coordinates in the middle of wavepacket propagation [22], as was done for the title reaction in Ref. [14], or use more complicated coordinate systems such as hyperspherical coordinates. A reactant-product decoupling (RPD) approach has recently been proposed which provides a general and efficient method for state-to-state dynamics calculations involving many product channels [23–26].

In the present study, however, we are primarily interested in total reaction probabilities and cross sections from given initial states and their energy dependence in order to study dynamical features of the title reaction such as resonance. Thus we simply use the reactant Jacobi coordinates to carry out the wavepacket propagation, and therefore the numerical treatment for the current calculation is essentially similar to that of a previous study for the $H + O_2$ reaction in Ref. [27]. Since $Li + HF \rightarrow LiF + H$ belongs to a light-heavy-light system with a near 90° skewing angle in the potential contour plot, the Jacobi coordinates are more or less equivalent to the bond lengths and bond angle coordinates. For an ideal (infinitely heavy central atom) light-heavy-light system, the product Jacobi coordinates differ from those of the reactant by a simple exchange of two bond lengths. Thus the treatment of Ref. [27] using the reactant Jacobi coordinates is very efficient for such an application. In the following, we give a brief summary of the necessary mathematical formulas.

For a fixed total angular momentum J, the Hamiltonian of an atom-diatom system can be expressed in terms of the Jacobi coordinates of the reactant arrangement A + BC,

$$H = -\frac{\hbar^2}{2\mu_R}\frac{\partial^2}{\partial R^2} + \frac{(\boldsymbol{J}-\boldsymbol{j})^2}{2\mu_R R^2} + \frac{\boldsymbol{j}^2}{2\mu_r r^2} + V(\mathbf{r},\mathbf{R}) + h(r), \quad (1)$$

where μ_R is the reduced mass between the center-of-mass of BC and A, $\boldsymbol{J}$ the total angular momentum operator of the system, $\boldsymbol{j}$ the rotational angular momentum operator of BC, and μ_r the reduced mass of BC. Here, we associate A with Li, B with F, and C with H. The diatomic reference Hamiltonian $h(r)$ is defined as

$$h(r) = -\frac{\hbar^2}{2\mu_r}\frac{\partial^2}{\partial r^2} + V_r(r), \quad (2)$$

where V_r is a diatomic reference potential (usually chosen as an asymptotic diatomic potential). The time-dependent wavefunction $\Psi(t)$ satisfying the Schrödinger equation can be expanded in terms of the BF (body-fixed) translational-vibrational-rotational basis [27] $\{u_n^v(R)\phi_v(r)Y_{jK}^{JM\epsilon}(\hat{R},\hat{r})\}$ as

$$\Psi_{r,v_0 j_0 K_0}^{JM\epsilon}(\mathbf{R},\mathbf{r},t) = \sum_{n,v,j,K} F_{nvjK,v_0 j_0 K_0}^{JM\epsilon}(t) u_n^v(R)\phi_v(r) Y_{jK}^{JM\epsilon}(\hat{R},\hat{r}), \quad (3)$$

where n is the translational basis label, M is the projection quantum number of J on the space fixed z axis, (v_0, j_0, K_0) denotes the initial rovibrational state, and ϵ is the parity of the system defined as $\epsilon = (-1)^{j+L}$, with L being the orbital angular momentum quantum number.

The $Y_{jK}^{JM\epsilon}$ in Eq. (3) is the BF total angular momentum eigenfunction defined as

$$Y_{jK}^{JM\epsilon} = (1+\delta_{K0})^{-1/2}\sqrt{\frac{2J+1}{8\pi}} \\ [D_{K,M}^{J} + \epsilon(-1)^{J+K} D_{-K,M}^{J}] y_{jK}, \tag{4}$$

where $D_{K,M}^{J}(\Theta\Phi\Psi)$ is the Wigner rotation matrix [28] with three Euler angles($\Theta\Phi\Psi$), y_{jK} are spherical harmonics, and ϵ is the parity of the triatomic system.

The functions $\phi_v(r)$ are eigenfunctions of the diatomic Hamiltonian of Eq. (2). The definition of the nondirect product basis functions $u_n^v(R)$ follows that in Ref. [20]

$$u_n^v(R) = \begin{cases} \sqrt{\frac{2}{R_4-R_1}}\sin\frac{n\pi R}{R_4-R_1} & v \le v_{\text{asy}} \\ \sqrt{\frac{2}{R_2-R_1}}\sin\frac{n\pi R}{R_2-R_1} & v > v_{\text{asy}}, \end{cases} \tag{5}$$

where v_{asy} is chosen to be the number of energetically open vibrational channels plus a few closed vibrational channels of the reagent HF. For the sake of clarity, we omit the labels $v_0 j_0 K_0$ and $JM\epsilon$ in the following discussion.

The propagation of the TD wavefunction is carried out by the split-operator scheme as [29],

$$\Psi_r(\mathbf{R},\mathbf{r},t+\Delta) = e^{-iH_0\Delta/2}e^{-iU\Delta}e^{-iH_0\Delta/2}\Psi_r(\mathbf{R},\mathbf{r},t), \tag{6}$$

where the reference Hamiltonian H_0 is defined as,

$$H_0 = -\frac{\hbar^2}{2\mu_R}\frac{\partial^2}{\partial R^2} + h(r), \tag{7}$$

and the effective potential operator U in Eq. (6) is defined as

$$U = \frac{(\boldsymbol{J}-\boldsymbol{j})^2}{2\mu_R R^2} + \frac{\boldsymbol{j}^2}{2\mu_r r^2} + V(R,r,\theta) \\ = V_{\text{rot}} + V \tag{8}$$

The matrix version of Eq. (6) for the expansion coefficient vector $\mathbf{F}$ is then given by

$$\mathbf{F}(t+\Delta) = e^{-i\mathbf{H}_0\Delta/2}e^{-i\mathbf{U}\Delta}e^{-i\mathbf{H}_0\Delta/2}\mathbf{F}(t) \tag{9}$$

and the operator $e^{-i\mathbf{U}\Delta}$ is further split as

$$e^{-i\mathbf{U}\Delta} = e^{-i\mathbf{V}_{\text{rot}}\Delta}e^{-i\mathbf{V}\Delta}e^{-i\mathbf{V}_{\text{rot}}\Delta}, \tag{10}$$

where $\mathbf{V}_{\text{rot}}$ is diagonal in the angular momentum basis representation and V is diagonal in coordinate representation [20].

The initial wavepacket is chosen as the product of a specific rovibrational eigenfunction and a localized translational wave packet,

$$\Psi_i(0) = \varphi_{k_0}(R)\phi_{v_0 j_0}(r)Y_{j_0K_0}^{JM\epsilon}(\hat{R},\hat{r}), \tag{11}$$

where the wavepacket $\varphi_{k_0}(R)$ is shaped by a standard Gaussian function

$$\varphi_{k_0}(R) = \left(\frac{1}{\pi\delta^2}\right)^{1/4}\exp[-(R-R_0)^2/2\delta^2]e^{-ik_0R}. \tag{12}$$

The exact rovibrational function $\phi_{v_0 j_0}(r)$ of HF is expanded in terms of the reference vibrational functions $\phi_v(r)$ to generate the coefficient vector of the wavefunction at $t=0$.

From the time propagation of the wavefunction, we can obtain the corresponding stationary scattering wavefunction ψ_{iE}^{+} and can calculate the total reaction probability from a specific initial state i by using the flux formula

$$P_i^R = \sum_f |S_{fi}^R|^2 = \langle\psi_{iE}^{+}|\hat{F}|\psi_{iE}^{+}\rangle, \tag{13}$$

where $\hat{\text{F}}$ is the flux operator. The above equation is evaluated as

$$P_i^R(E) = \frac{\hbar}{\mu_r}\text{Im}\left[\langle\psi_{iE}^{+}|\delta(r-r_0)\frac{\partial}{\partial r}|\psi_{iE}^{+}\rangle\right] \tag{14}$$

where the dividing surface for flux calculation is chosen at $r=r_0$. The TI scattering wavefunction can be obtained by performing a Fourier transform

$$\left|\psi_{iE}^{+}\right\rangle = \frac{1}{a_i(E)}\int_{-\infty}^{\infty} e^{\frac{i}{\hbar}(E-H)t}\left|\psi_i(0)\right\rangle \text{d}t \tag{15}$$

where the coefficient $a_i(E)$ is obtained from the projection of the initial wavepacket onto the asymptotic state [20, 27]

$$a_i(E) = \langle\Psi_{iE}^{+}|\Psi_i(0)\rangle \\ = \lim_{t\to-\infty} \\ \langle\phi_{iE}|e^{\frac{i}{\hbar}H_0t}e^{-\frac{i}{\hbar}Ht}|\varphi_i(0)\rangle = \langle\phi_{iE}|\varphi_i(0)\rangle, \tag{16}$$

where the last equation holds because the initial wave packet $\psi_i(0)$ is chosen to be located in the asymptotic region with only an incoming wave. The radial component of the free wavefunction has the asymptotic form

$$\phi_{iE}(R) = -\frac{\exp(-ik_iR)}{\sqrt{v_i}} + \frac{\exp(ik_iR)}{\sqrt{v_i}} = \frac{2i}{\sqrt{v_i}}\sin(k_iR), \tag{17}$$

for $J=0$ and is proportional to the spherical Ricatti-Bessel function for nonzero J. The free function has the same normalization as the full scattering wavefunction ψ_{iE}^{+}, namely, $\langle\phi_{iE}|\phi_{iE'}\rangle = 2\pi\hbar\delta(E-E')$.

After the reaction probabilities $P_i^R(E)$ have been calculated for all fixed angular momenta J, we can evaluate the reaction cross section for a specific initial state by simply summing the reaction probabilities $P_{v_0 j_0 K_0}^{J\epsilon}$ over all the partial waves (total angular momentum J),

$$\sigma_{v_0 j_0}(E) = \frac{\pi}{k_{v_0 j_0}^2}\sum_J (2J+1)P_{v_0 j_0}^J(E) \tag{18}$$

where $k_{v_0 j_0}$ is the wavenumber corresponding to the initial state for fixed energy E. In the present calculation, reaction probabilities for $J>1$ are calculated by employing the CS approximation [30], which is a common approximation employed in the calculation of cross sections.

3 Results and discussion

The numerical parameters used in the present TD calculation are as follows. A total of 150 sine basis functions are used to span a range of [1.5, 20.0] bohr in the R coordinate, 35 HF vibrational functions in the r coordinate, and 30 angular basis functions in the θ coordinate. Absorbing potentials are placed at the edge of both r and R grids and a time step of 10 atomic units is used for the wavepacket propagation in the split operator propagation. The center of the initial wavepacket sits at 15.0 bohr with a width of 0.45 bohr and an average kinetic energy of 0.07 eV and 0.25 eV for calculating reaction probabilities in the collision energy range of [0.001, 0.1] eV and [0.1, 0.4] eV, respectively.

Figure 2 shows reaction probability of $Li + FH \rightarrow LiF + H$ from the ground state of HF as a function of collision energy below 0.05 eV. In order to map out the entire resonance structure within this energy range, we used an energy resolution of 0.0001 eV to generate the plot in Fig. 2. Thus Fig. 2 contains probabilities for about 500 energies, all of which are calculated from the propagation of a single initial wavepacket! These results are obtained after propagating the wavepacket to about 10 ps, which is about the resolution limit of the energy data point. The resonance structure in Fig. 2 is converged with respect to further propagation of the wavepacket.

The most interesting dynamical feature in Fig. 2 is the complete dominance of the reaction probability by resonances, as reflected in the energy dependence of the reaction probability. As shown by sharp spikes in Fig. 2, the reaction probability suddenly rises to large values (as much as 0.4 or larger) when the collision energy hits one of the presumed resonance energies. At off-resonance energies, however, the reaction probability abruptly drops toward zero. In other words, there is essentially no direct reaction at such low collision energies and the reaction is completely controlled by reactive resonances which serve as gatekeepers for the reaction. This is because the collision energies in Fig. 2 are well below the reaction barrier and direct collisions at these low energies are essentially nonreactive. Thus the $Li + FH$ reaction is primarily determined by the resonance component of the initial wavepacket that decays to the LiF product. This explanation is supported by the fact that the probability function in Fig. 2 requires up to 10 ps of propagation time to converge and there are no sharp spikes at short propagation times. To examine further the effect of resonances, we show in Fig. 3 a contour plot of one of the resonance wavefunctions at $E = 0.2848$ eV (which corresponds to 0.0287 eV of collision energy). As is clear from Fig. 3, this resonance wavefunction is localized in the well of the $Li + FH$ entrance channel. The time propagation of this resonance wavefunction used as an initial wavepacket shows that a small fraction of the packet decays to the product channel $H + LiF$.

As collision energy increases to above 0.1 eV, the dynamics of the reaction changes qualitatively. As shown in Fig. 4, the reaction probability above 0.1 eV shows a broad background, implying a direct reaction process. However, resonance features are still clearly present and they are superimposed on the broad back-

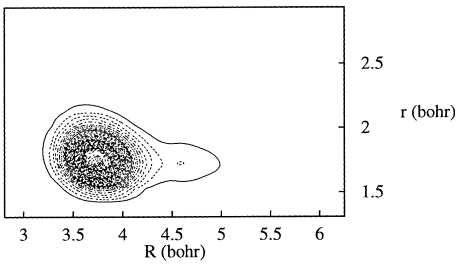

Fig. 3. Contour of a resonance wavefunction ($E_r = 0.2848$ eV with respect to the HF asymptote) as a function of two radial Jacobi coordinates R (between Li and the center of HF) and r (HF distance)

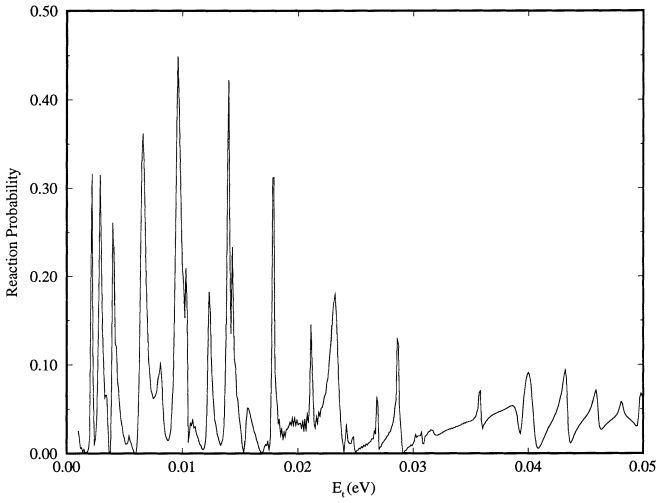

Fig. 2. Total reaction probability from the ground state of the HF reactant for $Li + HF \rightarrow LiF + H$ as a function of collision (translational) energy below 0.05 eV

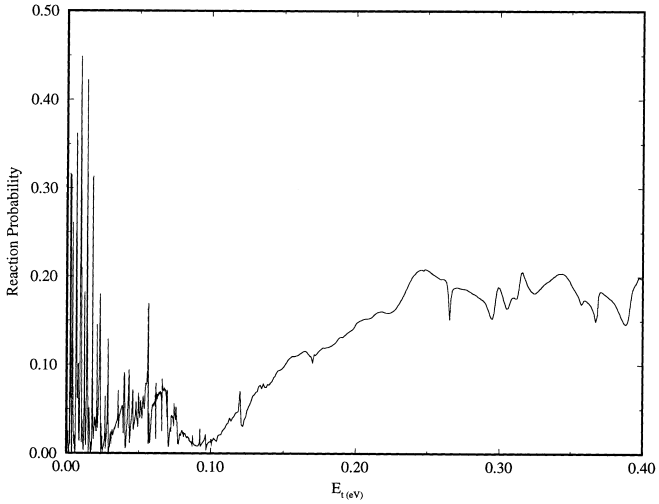

Fig. 4. Total reaction probability from the ground state of the HF reactant for $Li + HF \rightarrow LiF + H$ as a function of collision energy up to 0.4 eV

ground as small oscillations and spikes. This change of dynamical behavior is reflected in the process of TD propagation in which the broad background feature in Fig. 4 is converged within a few hundred femtoseconds while the features of small oscillations require propagation to a couple of picoseconds to be resolved. Thus resonance lifetimes at energies above 0.1 eV are on the order of 1 ps and the direct reaction process plays an important role at higher energies. Again, we see that TD calculation provides excellent rationales for understanding and explaining the dynamical features of the calculated results.

Baer et al. [15] have calculated reaction probabilities below the collision energy of 0.13 eV on the same PES. However, the sharp resonance feature in Fig. 2 is missing from their calculation. This is perhaps due to the sparsity of the energy points calculated and/or approximations used in the numerical calculation of Ref. [15]. The calculation of Parker et al. [5] reported reaction probabilities in the energy range of 0.004 to 0.35 eV, and their calculated resonance feature is quite similar to the present result. However, the dynamics calculation of Ref. [5] was done on a relatively coarse energy grid (0.0005 eV versus 0.0001 eV in the present calculation). Our calculation shows that an energy grid of 0.0005 eV is too coarse to produce *quantitatively* the resonance structure in Fig. 2. In particular, since an energy resolution of 0.0005 eV is limited to resolving resonances with maximum lifetimes about 3 ps, narrower resonances with longer lifetime must have been missed in the calculation of Ref. [5]. It is entirely possible that even the present calculation may have missed some resonances with lifetimes much longer than 10 ps. The most recent TD calculation by Gogtas et al. [14] has reported reaction probabilities in the energy range of 0.13 to 0.4 eV. This TD calculation produced reaction probabilities on a very dense energy grid, but the entire resonance feature below 0.13 eV is completely missed in this calculation [14]. However, for energies above 0.13 eV, our result agrees very well with that of Ref. [14], indicating good convergence of both calculations in this energy range.

In order to investigate the effect of initial states on reaction, we also calculated reaction probabilities for initial rotational states of HF at $j = 0$–3. There is a sensitive dependence of reaction probability on initial rotational state as shown in Fig. 5. In particular, rotationally excited HF generally gives larger reaction probabilities than does the ground rotation of HF. There is an interesting trend in that the even$-j$ probabilities generally rise and reach a common plateau, while odd$-j$ probabilities first decrease and then increase as a function of energy as shown in Fig. 5. We also note in Fig. 5 that reaction probabilities for different initial rotational states of HF all tend to converge near a collision energy of 0.26 eV. These results are in good agreement with the TD calculation of Gogtas et al. [14].

We next calculate the integral cross section from the initial ground state of HF. The calculations for $J > 0$ are done using the CS approximation [30]. We calculated reaction cross sections from the ground state of HF for energies above 0.10 eV because calculation of cross section at lower collision energies would take much longer computer time due to long-lived resonances, as discussed above. The calculation of the cross section is done for J up to 52 in order to converge the result for collision energies up to 0.4 eV. The most interesting feature in the calculated cross section is perhaps the presence of a broad maximum around 0.26 eV, as shown in Fig. 6. In addition, there are small oscillations superimposed on the broad background of the cross section, indicating resonance features present in the underlying reaction probabilities for each individual partial wave J. A comparison of cross section with experimental measurement is also given in Fig. 6, where we see that the theoretical result is smaller than the experimental measurement. However, we should bear in mind that the experimental cross section involves thermal averaging over initial rotational states of HF, while

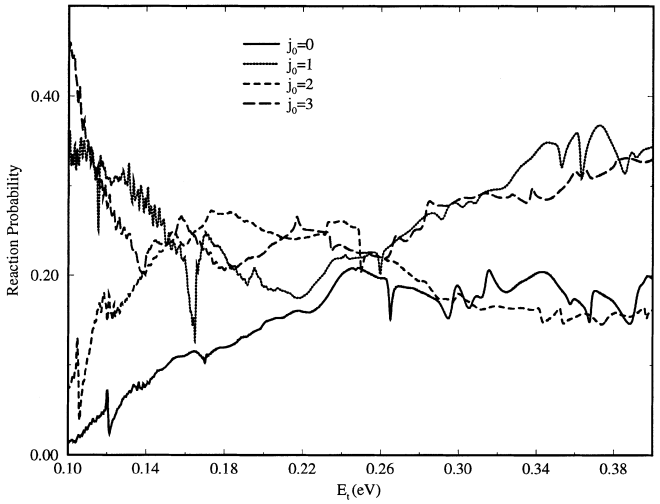

Fig. 5. Total reaction probabilities from rotational states $j = 0, 1, 2, 3$ of the HF reactant for Li + HF → LiF + H as a function of collision energy up to 0.4 eV. *Solid line* is for $j = 0$, *dotted line* for $j = 1$, *dashed line* for $j = 2$, and *dot-dashed* line for $j = 3$

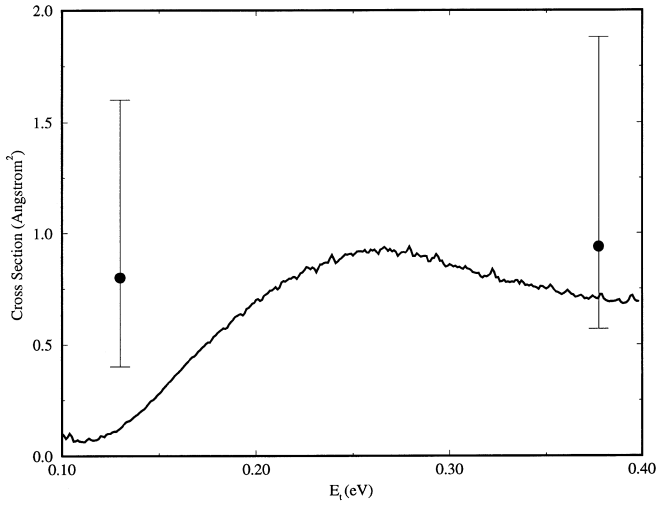

Fig. 6. Integral cross section from the ground state of the HF reactant for Li + HF → LiF + H as a function of collision energy between 0.1 and 0.4 eV. The experimental values are from Ref. [7]

the present theoretical cross section is calculated for the ground rotational state of HF only. In view of the enhancement of reaction probability by initial rotational excitation of HF for total angular momentum $J = 0$, as shown in Fig. 5, it is reasonable to expect that the theoretical cross section for excited rotational states of HF would be larger than that of the ground state. In particular, we speculate that rotation-excited cross sections would likely be much larger mainly for energies below and above 0.26 eV, based on the results in Fig. 5, where probability curves of different initial rotational states tend to converge near the energy of 0.26 eV. Baer et al. [15] calculated cross sections below the energy of 0.13 eV and therefore no comparison can be made between the present cross section and that of Ref. [15]. Neither Parker et al. [5] nor Gogtas et al. [14] calculated cross sections for Li + HF reaction.

In order to help gain physical insight into the appearance of the maximum in the energy-dependence of integral cross section, we show in Fig. 7 the $J_{\max}$ dependence of cross section which is obtained by summing over total angular momentum J in Eq. (18) up to a maximum value $J_{\max}$ for various values of $J_{\max}$. It is seen that major contributions to the cross section are from reaction probabilities with J values in the range 20–40. The cross section remains generally flat until after summing over $J_{\max}$ above 30. We see also from Fig. 7 that the small oscillations on the curve of cross section mainly come from reaction probabilities near and greater than $J_{\max} = 20$.

We also use the J-shifting approximation [17] to estimate the cross section as given by

$$\sigma_{v_0 j_0}(E)_{\text{shift}} \approx \frac{\pi}{k^2_{v_0 j_0}} \sum_J (2J+1) P^{J=0}_{v_0 j_0}[E - B^{\#} J(J+1)], \tag{19}$$

where the value of rotation constant $B^{\#}$ is taken from Ref. [16] ($B = 5.721 \times 10^{-6}$ au). As shown in Fig. 8, the

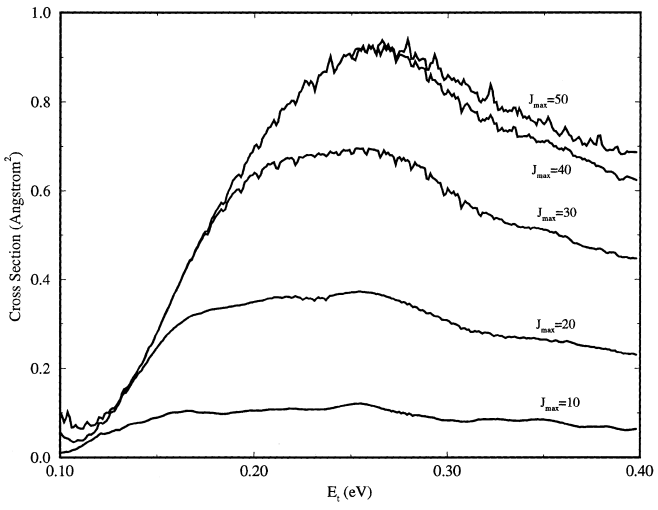

Fig. 7. $J_{\max}$ dependence of the integral cross section, where $J_{\max}$ is the maximum value of total angular momentum J used in the summation of Eq. (18)

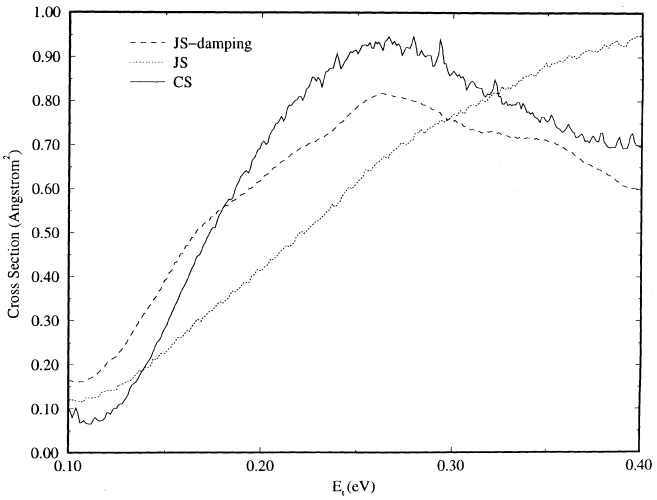

Fig. 8. Integral cross sections obtained from the present CS calculation (*solid line*), simple J-shifting calculation (*dotted line*), and improved J-shifting calculation (*dashed line*)

J-shifting cross section is a monotonically increasing function of energy. This result is very similar to that of an earlier J-shifting calculation by Lagana et al. [16], which also gave a monotonically increasing cross section with energy. Since the reaction probability at low energies for $J = 0$ is highly oscillatory, the straightforward application of the J-shifting technique will produce a highly oscillatory cross section as a function of energy. The smoother J-shifting cross section in Fig. 8 is obtained by cutting off the $J = 0$ reaction probability for energies below 0.1 eV in Eq. (19). This is justified by our calculations of reaction probabilities for higher values of total angular momentum J in which the sharp resonance structure in Fig. 2 is absent in reaction probabilities for higher J values. The physical picture for the lack of such sharp resonances in higher J reactions is the following: the shallow well in the entrance channel where low-energy resonances are located is being filled up by the centrifugal potential $J(J+1)/2\mu R^2$, and this eliminates many narrow resonances at low collision energies.

A comparison of two cross sections in Fig. 8 shows clearly that the J-shifting approximation using the value of Ref. [16] underestimates the cross section in the middle energy but overestimates the cross section at high energies. We also used a different value of $B^{\#}$ to obtain the J-shifting cross section, but the result is qualitatively similar. In order to understand the failure of J-shifting approximation, we plot reaction probability vs J for various values of J up to $J = 50$ in Fig. 9. We observe in Fig. 9 that the amplitude of the probability curve gradually decreases as J increases for $J \geq 20$. Thus the reaction probability falls off for high values of J. In the J-shifting approximation, however, the amplitude of the reaction probability for all values of J is assumed to be the same as that for $J = 0$. In view of this observation, it might be tempted to try to improve the J-shifting approximation by including a damping function $F(J)$ in the summation over J

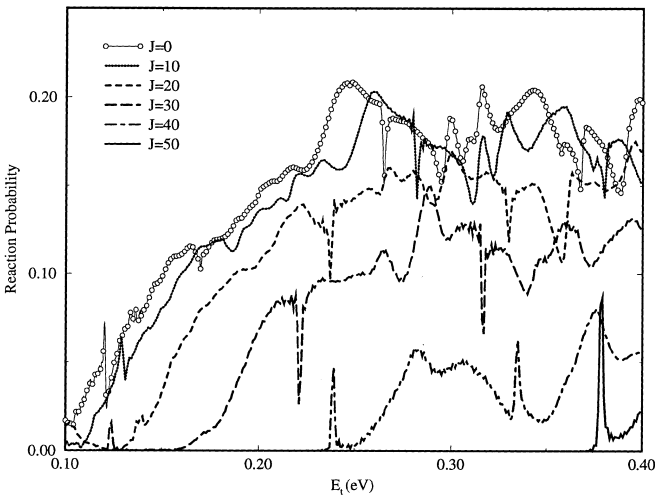

Fig. 9. Total reaction probability from the ground state of the HF reactant for $Li + HF \rightarrow LiF + H$ as a function of collision (translational) energy for several values of total angular momentum J

$$\sigma_{v_0 j_0}(E)_{\text{shift}} \approx \frac{\pi}{k^2_{v_0 j_0}} \sum_J (2J+1) P^{J=0}_{v_0 j_0}[E - B'^{\#} J(J+1)] F(J) \quad \text{for } J > 20, \tag{20}$$

where $F(J)$ is a decreasing function of J. We tried the following damping function:

$$F(J) = \exp[-\alpha J(J+1)]. \tag{21}$$

Here, we used the value of $B'^{\#} = 2.135 \times 10^{-6}$ au and $\alpha = 0.001$, and the result is plotted in Fig. 8. As is seen, the resulting J-shifting cross section is significantly improved and has reproduced the maximum between 0.2 and 0.3 eV.

4 Conclusion

We report detailed quantum dynamics studies for $Li + HF$ reaction using a TD wavepacket approach. Initial state-selected reaction probabilities are computed for several rotational states of the reagent for collision energies below 0.4 eV. The reaction at energies below 0.1 eV is dominated by resonances. In particular, reaction at collision energies below 0.05 eV is completely controlled by resonances and the direct reaction process is negligible (probability at off-resonance energy is essentially zero). The lifetimes of these low-energy resonances generally fall in the range 1–10 ps. The plots of resonance wavefunctions show that these low-energy resonances are mainly localized in the potential well of the $Li + HF$ entrance channel. At collision energies above 0.1 eV, the reaction probabilities show broad background with some resonance features superimposed on that. There is a sensitive dependence of reaction probability on the initial rotational state of the reagent. In particular, the even and odd rotation states of HF give qualitatively different energy dependence of probabilities. These results are generally in good agreement with those of Gogtas et al. [14] and those of Parker et al. [5] in their respective energy range.

The integral cross section calculated using the CS approximation shows small oscillations superimposed on a broad background and is reminiscent of the underlying resonances in individual J-fixed reaction probabilities. One interesting dynamical feature from our calculation is that the energy dependence of the cross section exhibits a broad maximum near the collision energy of 0.26 eV. This feature is absent in the cross section obtained by applying the simple J-shifting technique which gives a monotonically increasing cross section with collision energy. However, improved J-shifting approximation by using a decaying function of J gives a much better result and is capable of reproducing the maximum in the energy dependence of the cross section. Our calculated cross sections from the ground state of HF are smaller than the rotation-averaged experimental values. However, the initial j dependence of reaction probability indicates that the agreement with experiment is expected to significantly improve on inclusion of theoretical cross sections from rotationally excited HF. In particular, we expect that the theoretically calculated rotation-averaged cross section will mostly likely "flatten up" from both side of the collision energy near 0.26 eV in Fig. 6.

Acknowledgements. We thank Russell Pack and Miguel Paniagua for sending us the code for LiHF PES. We also thank Donald G. Truhlar for careful reading of the manuscript as well as correction of errors. This work is supported by the Division of Chemical Sciences, Office of Basic Energy Sciences, Office of Energy Research, US Department of Energy, under Grant No. DE-FG02-94ER14453.

References

1. Balint-Kurti GG, Yardley RN (1977) Faraday Discuss Chem Soc 62: 77
2. Chen MML, Schaefer HF III (1980) J Chem Phys 72: 4376
3. Palmieri P, Lagana A (1989) J Chem Phys 91: 7303
4. Aguado A, Suarez C, Paniagua M (1995) Chem Phys 201: 107
5. (a) Parker GA, Lagana A, Crocchianti S, Pack RT (1995) J Chem Phys 102: 1238; (b) Parker GA, Pack RT, Lagana A (1993) Chem Phys Lett 202: 75
6. Bartoszek FE, Blackwell BA, Polanyi JC, Sloan JJ (1981) J Chem Phys 74: 3400
7. Becker CH, Casavecchia P, Tiedemann PW, Valentini JJ, Lee YT (1980) J Chem Phys 73: 2833
8. Loesch HJ, Ramscheid A, Stenzel E, Stienkemeier F, Wustenbecker B (1992) In: Mac-Gillvary WR, McCarty IE, Standage M (eds) Physics of electronic and atomic collisions. Hilger, Bristol, p 579; Loesch HJ, Stenzel E, Wustenbecker B (1991) J Chem Phys 95: 3841
9. Loesch HJ, Steinkemeier F (1993) J Chem Phys 98: 9570; 99: 9598
10. Alvarino JM, Casavecchia P, Gervasi O, Lagana A (1982) J Chem Phys 77: 6341; Alvarino JM, Hernandez ML, Garcia E, Lagana A (1986) J Chem Phys 84: 3059; Noorbatcha I, Sathyamurthy N (1982) J Chem Phys 76: 6447; Loesch HJ (1986) Chem Phys Lett 104: 213
11. Miller DL, Wyatt RE (1987) J Chem Phys 86: 5557
12. (a) Lagana A, Garcia E (1987) Chem Phys Lett 139: 140; (b) Lagana A, Garcia E, Gervas O (1988) J Chem Phys 89: 7238; (c)

Baer M, Garcia E, Lagana A, Gervasi O (1989) Chem Phys Lett 158: 362
13. Balint-Kurti GG, Gogtas F, Mort SP, Offer AR, Lagana A, Garvasi O (1993) J Chem Phys 99: 9567
14. Gogtas F, Balint-Kurti GG, Offer AR (1996) J Chem Phys 104: 7927
15. (a) Baer M, Last I, Loesch HJ (1994) J Chem Phys 101: 9648; (b) Baer M, Loesch HJ, Werner HJ, Last I (1994) Chem Phys Lett 219: 372
16. Lagana A, Pack RT, Parker GA (1993) J Chem Phys 99: 2269
17. (a) Bowman JM (1985) Adv Chem Phys 61: 115; (b) Sun Q, Bowman JM, Schatz GC, Sharp JR, Connor JL (1990) J Chem Phys 92: 1677; (c) Mielko SL, Lynch GC, Truhlar DG, Schwenke DW (1993) Chem Phys Lett 216: 441
18. Neuhauser D, Baer M, Judson RS, Kouri DJ (1991) Comput Phys Commun 63: 460
19. Zhang DH, Zhang JZH (1993) J Chem Phys 99: 5615; *ibid* (1994) 100: 2697
20. Zhang DH, Zhang JZH (1994) J Chem Phys 101: 1146
21. (a) Neuhauser D, Baer M (1989) J Chem Phys 91: 4651; (b) Neuhauser D, Baer M, Kouri DJ (1990) J Chem Phys 93: 2499
22. Judson RS, Kouri DJ, Neuhauser D, Baer M (1990) Phys Rev A 42: 351
23. Peng T, Zhang JZH (1996) J Chem Phys 105: 6072
24. Kouri DJ, Hoffman DK, Peng T, Zhang JZH (1996) Chem Phys Lett 262: 519
25. Zhu W, Peng T, Zhang JZH (1997) J Chem Phys 160: 1742
26. Dai J, Zhang JZH (1997) J Chem Soc Faraday Trans 93 (in press)
27. Zhang DH, Zhang JZH (1994) J Chem Phys 101: 3671
28. Rose ME (1957) Elementary theory of angular momentum. Wiley, New York
29. Fleck JA Jr, Morris JR, Feit MD (1976) Appl Phys 10: 129
30. (a) Pack RT (1974) J Chem Phys 60: 633; (b) McGuire P, Kouri DJ (1974) J Chem Phys 60: 2488